ORIGINAL ARTICLE

Identification of Confounding Factors on 2-D Shear-Wave Elastography of Kager's Fat Pad: An *Ex-Vivo* Study

Abdalmalek Ismail Aburabee[1], Sook Sam Leong[2], Mohd Shukry Khalid[3], Noor Shafini Mohammad[4]

[1] Centre for Medical Imaging Studies, Faculty of Health Sciences, Universiti Teknologi MARA, 42300 Selangor, Malaysia.
[2] Centre of Medical Imaging, Faculty of Health Sciences, Universiti Teknologi MARA Selangor, Selangor, Malaysia.
[3] Department of Radiology, Faculty of Medicine, Universiti Teknologi MARA, 47000 Selangor, Malaysia.
[4] Medical Imaging, University of Exeter, EX1 2LU Exeter, United Kingdom

ABSTRACT

Introduction: To identify the confounding factors presented by Keger's fat pad (KFP) using 2-D shear-wave elastography (2-D SWE) in phantom. **Methods:** The study was conducted between January and June 2023. A total of eleven bovine ankles were scanned using various gel layers, scanning planes, ankle positions, and ROI sizes. The stiffness measurement (in m/s) of KFP for each ankle was acquired within a day. To assess interobserver reliability, seven ankles were rescanned by a second observer. **Result:** Wilcoxon sign-rank test indicated a significant in shear wave velocity (SWV) between longitudinal and transverse plane ($p = 0.043$). A significant difference was observed in different gel layers ($p = 0.002$). The SWV was higher when the ROI diameter was 3.0 mm compared to 1.0 mm ($p < 0.001$). Insignificant difference was also observed in different ankle positions ($p = 0.756$). The coefficient variance was low-er in longitudinal, one-layer gel, with an ROI of 1.0 mm and in neutral position with ($p < 0.05$). For interobserver reliability, the intraclass correlation coefficient (ICC) was 0.819 (95% CI, 0.737–0.875) for the proposed protocol. The ICC between the two machines was 0.746 (95 % CI, 0.625 - 0.827) with the Bland Altman test indicating no proportional bias ($p = 0.519$). SWV in fat pad is affected by the scanning plane, gel layers, and ROI size. **Conclusion:** Using a standard scanning protocol, 2-D SWE can produce reliable images even with different scanners.
Malaysian Journal of Medicine and Health Sciences (2025) 21(6):1-8. doi:10.47836/mjmhs.v21.i6.1368

Keywords: Confounding factors, Kager's fat pad, Reliability, Shear-wave elastography, Shear-wave velocity

Corresponding Author:
Sook Sam Leong, PhD
Email: sam_leong10284@icloud.com
Tel: +60129307153

INTRODUCTION

Musculoskeletal (MSK) disorders are the second most common health of issue globally, particularly affecting adolescents and young adults, with a higher incidence observed in males during sports activities and females during daily or occupational activities, accounting for 40% of all injuries (1). The most common is ankle injury according to Zhang et al. (2), acute ankle sprains account for 15–20% of all sports-related injuries, besides being the most prevalent lower limb injury among athletes. There is no clear connection, but prolonged ankle instability following acute sprain has reportedly led to chronic problems with gait, foot posture and minor changes in Achilles tendon mechanics. The KFP plays a key biomechanical and protective role within the posterior ankle, acting as a cushion between adjacent structures such as the Achilles tendon, flexor hallucis longus, and calcaneus, furthermore, participate in joint lubrication. Clinically, posterior ankle pain can result from various conditions. Identifying inflammation in KFP through imaging can help narrow the differential diagnosis and guide targeted treatment. These modifications may have an indirect relation with the distribution of loads surrounding the KFP, also known as the pre-Achilles fat pad, which could lead to changes in the pad's density or appearance over time (3).

Due to its close anatomical relationship with the Achilles tendon, fat pad is sensitive to inflammation caused by trauma, infection, or tumours at the Achilles tendon. Such conditions can impact the integrity and functionality of the fat pad (4,5,6). Inflammation of fat pad can be diagnosed through imaging methods such as magnetic resonance imaging (MRI) and conventional

ultrasound. Undoubtedly, conventional ultrasound is an irreplaceable modality. in different settings due to multiple benefits like being non-invasive, portable, and affordable (5,7). It can detect changes in the fat pads' atypical lobular pattern when there is soft tissue inflammation (8). However, when it comes to assessing MSK disorders, conventional ultrasound has limitations. The accuracy varies depending on the operators' level of competence in interpreting the images (9). Hence, new imaging tools are required to diagnose pathologies effecting fat pad. Tissue mechanical characteristics are altered in diseased circumstances, and shear-wave elastography (SWE) can quantify pathologies in terms of stiffness [kilopascals (kPa)] or wave velocity [meters per second (m/s)] travelling through the tissue in response to mechanical stress (10). Authors have studied SWE in human tendons, ligaments, and muscles with promising results (11.12). However, despite the considerable attention given to the Achilles tendon in published literature, there remains a notable gap in research concerning the evaluation of KFP using SWE. To date, no studies have utilised SWE to assess stiffness of fat pad. Consequently, there is a lack of consensus regarding the typical range of stiffness observed in healthy fat pad tissues. This gap underscores the need for further investigation into the biomechanical properties of fat pad and its potential implications for ankle joint health. Yet, a uniform scanning technique for fat pad using SWE should be developed before a general reference value for normal fat pad is established. Therefore, this study aims to identify the possible confounding factors presented by fat pad using 2-D SWE.

MATERIALS AND METHODS

Study design and samples

The study was divided into two sections: the confounding variables investigation and the protocol reliability study. The study was accomplished in accordance with the Declaration of Helsinki and approved by the Research Ethics Committee (REC/08/2023 (PG/MR/282)).

Based on earlier studies examining the behaviour of the fat pad in bovine, it exhibits similar biomechanical properties to human pre-Achilles fat pad (6,13,14). Thus, bovine ankles were used in this study for better understanding of the mechanical characteristics and behaviour of fat pad under controlled circumstances. This experimental study was conducted between January and June 2023. Each ankle was scanned within a day. A total of eleven bovine ankles were purchased from a local abattoir for this study.

Confounding factor study

Two trained observers with prior experience in ultrasound participated in the scanning procedures. Both observers used the same ultrasound machine and monitor SWE Samsung RS85 Prestige system equipped with the S-Shearwave software (Samsung Medison Co., Seoul, Korea) and LA2-9A linear array transducer with frequency range of 2.0 - 9.0 MHz. All phantoms were scanned.. by the first operator (A.M.A.R) with three years' experience in ultrasound. During SWE imaging, the transducer was positioned steadily at the posterior aspect of the bovine ankle where the fat pad was located, without applying compression. SWE were acquired once the reliability measurement index (RMI) achieved > 0.4, indicating the reliability of stiffness measurements. The KFP's SWV was measured in meters per seconed (m/s). Ten consecutive measurements were taken, and the median value was recorded. In this study we investigated some of the possible confounding factors: (i) the scanning plane, (ii) the layers of ultrasonic gel, (iii) region of interest (ROI), and (iv) variation in bovine ankle positioning. Specific details of the experimental setups for each of these factors are outlined in the subsequent sections.

Scanning plane

The bovine ankles were placed on the ultrasound table in a neutral position. One-layer of ultrasonic gel was applied to the posterior aspect where the fat pad was located. The longitudinal plane of the fat pad was identified in the midline. SWE was activated once the image was stabilised. A 1.0 mm diameter ROI was placed at the sagittal midline of the fat pad. Once the SWE images of the longitudinal plane of the fat pad were obtained, without sliding the probe, the probe was rotated in an anticlockwise direction by changing the scanning plane of the fat pad to the transverse plane. The SWV measurements were obtained in a transverse plane with a 1mm diameter ROI.

Ultrasonic gel layer

The bovine ankles were held in a neutral posture. One-layer of ultrasonic gel was applied to the posterior aspect of the ankle. SWE was activated once the fat pad longitudinal plane was in profile. A 1.0 mm diameter ROI was positioned at the fat pad at the sagittal midline for SWE image acquisition. Image acquisition was repeated using five-layers of ultrasonic gel.

ROI size

The bovine ankles were placed in a neutral posture with one-layer of ultrasonic gel applied. SWE was activated once the fat pad in the longitudinal plane was in profile. The ROIs were placed at five distinct locations within KFP, as shown in Figure 1. These locations were selected to provide a representative sampling across the anatomical extent of the fat pad. Care was taken to avoid adjacent anatomical structures such as the Achilles tendon and calcaneus to minimize measurement interference. The SWE image acquisition was repeated after changing the ROI size to 3.0 mm in diameter.

Ankle positioning

The bovine ankles were placed in a neutral position. One-layer of ultrasonic gel was applied to the ankle.

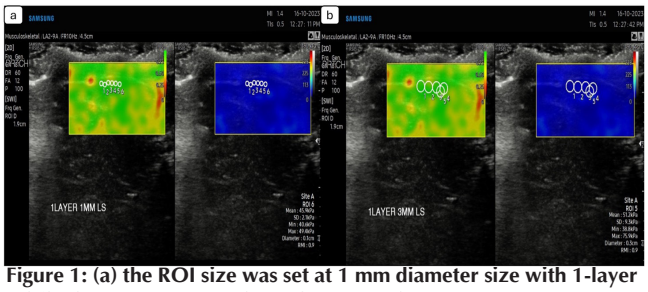

Figure 1: (a) the ROI size was set at 1 mm diameter size with 1-layer gel (b) the ROI size was adjusted to 3 mm diameter size. ROI=region of interest.

Once the sonographer could visualise the longitudinal plane of the fat pad, the SWE was activated. After the image became stabilised, an ROI with the size of 1.0 mm diameter was placed at the sagittal midline of the fat pad. The scans were repeated by positioning the ankle on a sponge to maintain a 30-degrees flexion (Figure 2).

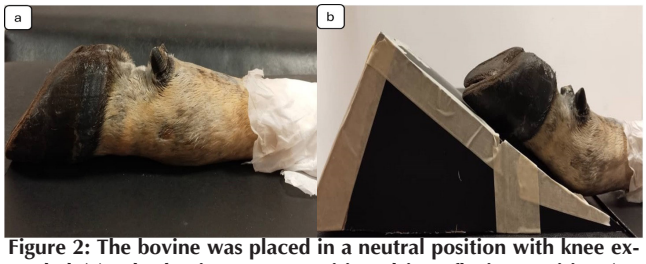

Figure 2: The bovine was placed in a neutral position with knee extended (a). The bovine was repositioned in a flexion position (30 degrees) (b). The bovine ankle was supported by sponge to maintain the ankle flexion in 30 degrees.

Protocol reliability study

Operator

The scanning protocol was established based on confounding factors that had lower coefficient of variations (CVs). Using the same Samsung ultrasound machine and transducer, a second operator (L. S. S.) with twenty years' experience in ultrasound on seven bovine ankles using the developed scanning protocol. The median measures of stiffness were calculated after the ten measurements were taken. Each observer independently performed the scans in separate sessions to minimize observational bias. During the image acquisition, only the performing observer was present in the scan room. The second observer was blinded to the measurements and scan results obtained by the first observer, without access to prior data or communication permitted between observers during the scanning process. The second observer performed the scans immediately after the first observer.

Ultrasound machine

Seven bovine ankles were rescanned by the first operator using a second ultrasound machine: the Toshiba Aplio i700 ultrasound scanner (Canon Medical Systems, Berlin, Germany) and an i18LX5 linear array transducer with a frequency range of 4.0 - 18.0 MHz. A total of ten measurements were acquired to calculate the median.

DATA ANALYSIS

Statistical analysis tests were conducted using SPSS version 28 (SPSS Inc, Chicago, Illinois, USA). The dataset demonstrated a mixed pattern of normality, where some variables were normally distributed while others were not, as assessed using the Shapiro-Wilk test. Given this variability, non-parametric statistical methods were deemed more appropriate for analyzing the data. Therefore, the Wilcoxon signed-rank test was applied to compare differences between conditions, ensuring the robustness of the statistical analysis. The coefficient of variation (CV) was calculated to assess the degree of variation in a dataset relative to SWE mean. For each method, ten repeated SWE measurements were obtained to calculate the CV, which reflects the degree of variability relative to the mean SWE value. The formula used to determine the CV is stated in Equation 1 (15).

$$CV = (\text{Standard deviation}/\text{Mean}) \times 100\ \% \qquad \text{(EQ. 1)}$$

An intraclass correlation coefficients (ICCs) with two-way mixed effects model was used to evaluate the reliability of the repeated measurements of each ROI acquired by different operators. ICC also used to evaluate the reliability of the repeated measurements of each ROI using different machine. The degree of agreement was quantified as poor (ICC<0.50), moderate (ICC 0.50–0.75), good (ICC 0.75–0.90): or excellent (>0.90). Bland Altman test was conducted to assess the agreement between machines. A p-value < 0.05 was considered statistically significant.

ETHICAL CLEARANCE

We obtained approval from the Research Ethics Committee (REC/08/2023 (PG/MR/282), Universiti Teknologi MARA.

RESULT

SWV from different scanning planes

Figure 3 illustrates the stiffness measurements of the fat pad in both the longitudinal and transverse planes. The Wilcoxon signed-rank test revealed that the median SWV measured in the transverse plane (6.48 m/s; IQR = 0.8

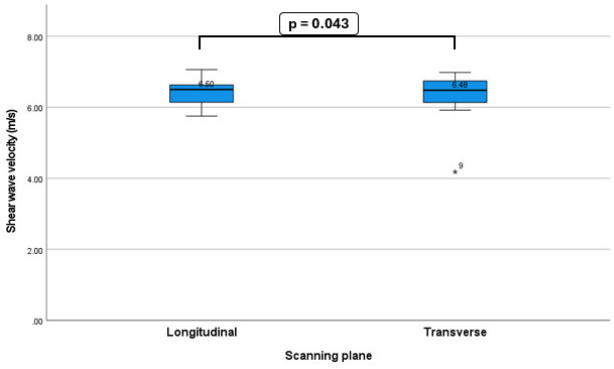

Figure 3: The median of SWV measurement in different scanning plane.

m/s) was significantly lower than that in the longitudinal plane (6.50 m/s; IQR = 0.9 m/s), (Z = -2.023, p = 0.043). The CV of the longitudinal plane measurements (85%) was significantly lower than that of the transverse plane (94%) (p = 0.042), suggesting relatively less variability in the longitudinal scans. However, the high CV values in both planes indicate substantial variability in the SWV measurements.

SWV from different layers of the ultrasonic gel

Figure 4 demonstrates the stiffness measurements of the fat pad using different layers of ultrasonic gel. The Wilcoxon signed-rank test showed that the SWV was significantly higher when a single layer of gel was applied compared to five layers. The median SWV for the one-layer method was 6.71 m/s (IQR = 0.7 m/s), whereas for the five-layer method, it was 5.81 m/s (IQR = 0.8 m/s), (Z = -3.109, p = 0.002). The CV in one-layer gel (68%) was significantly lower compared with five-layers (91%) (p = 0.001).

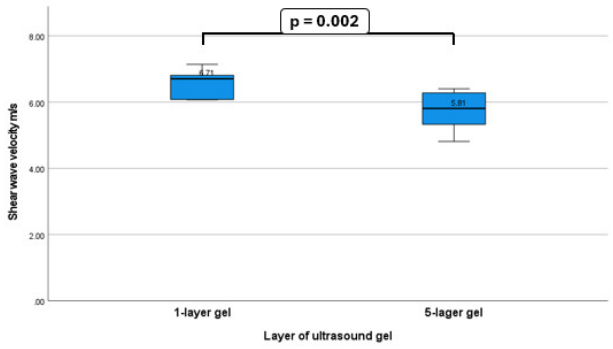

Figure 4: The median of SWV measurement scanning using different layer of ultrasonic gel.

SWV from different ROI sizes

Figure 5 illustrates the stiffness measurements of the fat pad using two ROI sizes: 1.0 mm and 3.0 mm in diameter. The Wilcoxon signed-rank test indicated that the SWV measured with the larger ROI (6.81 m/s, IQR = 0.9 m/s) was significantly higher than that measured with the standard ROI size (6.48 m/s, IQR = 0.7 m/s), (Z = -2.034, p < 0.001). The CV in the ROI size of 1.0 mm diameter (68%) was lower than that of 3.0 mm diameter (72%) (p = 0.010).

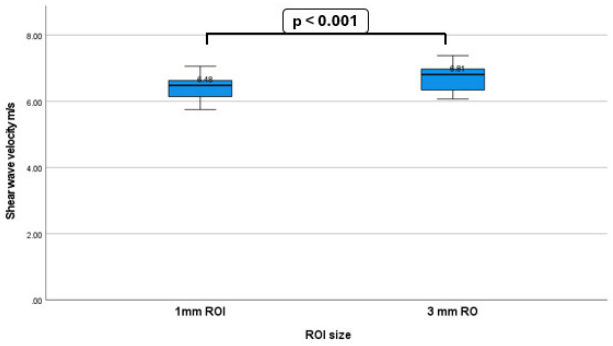

Figure 5: The median of SWV measurement using different ROI size. ROI=region of interest.

SWV from different ankle positioning

Figure 6 presents the fat pad stiffness measurements at two different ankle positions. The Wilcoxon signed-rank test revealed no significant difference in SWV between the positions. When the ankle was positioned at 30 degrees of plantarflexion, the median SWV was 6.29 m/s (IQR = 0.7 m/s), which was slightly lower than the neutral position, where the median was 6.48 m/s (IQR = 0.9 m/s), (Z = -0.310, p = 0.756). The CV for flexion (94%) was higher than neutral (89%) (p < 0.001).

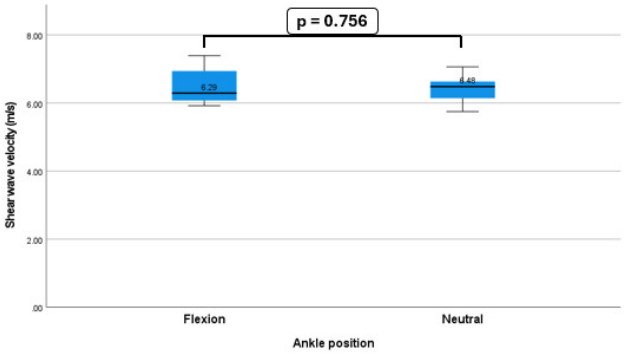

Figure 6: The median of SWV measurement at different ankle positions.

Inter-observer reliability of SWV measurements

The inter-observer reliability, the ICC was 0.819 (95% CI, 0.737–0.875) (p < 0.001). This indicated that the SWV measurements had good reliability and less error between the operators.

Inter-machine reliability of SWE measurements

A moderate inter-machine reliability between Samsung and Canon scanners was observed, in which the ICC was 0.746 (95 % CI, 0.625 - 0.827), (p < 0.001). Bland Altman test revealed no proportional bias (p = 0.519). These findings suggested that the two machines could provide measurements that were in good agreement, with consistent variability across the range of measurements (Figure 7).

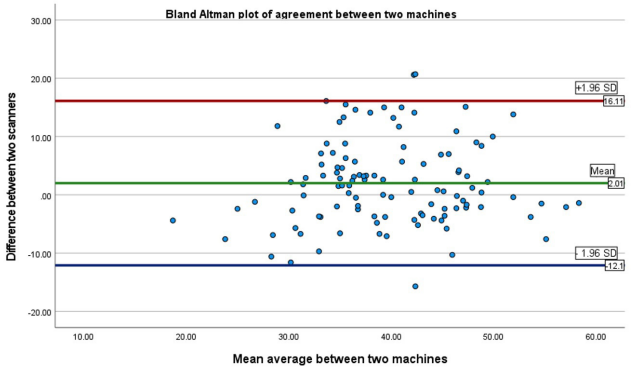

Figure 7: Bland Altman is showing the upper limit of agreement red line, mean dark green line.

DISCUSSION

By evaluating potential confounding variables during SWE imaging, this methodological investigation had determined the confounding factors in 2-D SWE of fat

pad. The results demonstrated that measured stiffness could be influenced by the scanning plane, amount of ultrasound gel and ROI size. One of the developments in elastography techniques is 2-D SWE, which allowed a quantitative evaluation of the medium stiffness in real-time (16). SWE could provide quantitative findings and colour elasticity maps with significant reproducibility (17). Pathological changes to musculoskeletal stiffness might manifest as either an increase in stiffness because of calcified or fibrotic tendon, or a decrease in stiffness because of disruption to the organised extracellular matrix structure (17). Studies had recently demonstrated that by measuring changes in stiffness, SWE could precisely diagnose an inflamed muscle and tendon. Thus, it could be used in diagnosing MSK disease in addition to conventional ultrasonography. However, there were limited studies investigating the confounding factors that potentially increased the variability of measured SWV (18). To date, no study had utilised SWE in fat pad.

Gennisson et al. (19), found that shear waves propagated much faster along muscle fibers compared with perpendicular direction or at any interval of rotation therein. Later investigations supported these initial findings, as longitudinal transducer orientations obtained the most reliable measures of muscle elasticity (20,21). Wang et al. (22) concluded that shear wave travelled poorly in tissue with high anisotropy levels, such as muscles and tendons. When the shear wave propagated perpendicular to the tendon fiber direction, its velocity is repeatability lower. The fat pad is an adipose structure with fibrous bands that are distributed in a varied way between the surrounding tissues (4). As highlighted in the study by Sun et al. (23), adipose tissue was found to be anisotropic, thus, this explained the significant difference in scanning planes of the fat pad. As a result, when taking fat pad measurements, it is essential to standardise the scanning plane. In this study, we observed that the transverse plane offered less consistent readings. This was likely due to pre-compression by the operator. According to Kot et al. (24), increased transducer pressure would increase in the observed elastic modulus for muscles. Image acquisition in the transverse plane was complicated due to echogenicity alteration. Thus, the operator could have applied more pressure to obtain a better image quality for SWE acquisition.

Elastography technology often requires a distance between the structure of interest and the skin's surface when calculating stiffness. Because of this, the application of SWV on superficial structures such as KFP might be complicated. Researchers had investigated how much gel to use in an examination, such as 0.5 cm or 2.5 cm thickness (18), and also a generous amount (25). In this study, we investigated the effects of ultrasonic gel layers applied on SWE image acquisition. According to our findings, there was a significant difference in SWV measurements when scanning with one-layer and five-layer gels. Based on our findings, the one-layer gel produced more consistent SWV measurements and lower variability, indicating better reproducibility. Therefore, one-layer gel is preferred due to its superior signal consistency and reduced artifacts from transducer pressure. Higher measurement variability found in five-layers of gel could be due multiple layers increase the distance between the transducer and the target tissue, creating a "lever arm" effect that reduces fine motor control (26). This added distance makes it more difficult to maintain steady contact with the scanning surface. As a result, hand instability becomes more pronounced, leading to image inconsistency. Since SWE is highly sensitive to motion and probe stability, even slight variations in hand position can significantly affect stiffness measurements and compromise reproducibility (27). According to Prado-Costa et al. (28), ultrasound elastography equipment required a minimum distance of 1-2 mm between the structure of interest and the surface of the skin for the calculation of the elastogram. While the minimum needed distance had been met using one-layer gel, we observed that the use of five-layer gel provided less consistent results than one-layer gel. Moreover, we found that the ultrasound image quality was better and that obtaining sufficient elastography images required less effort when one-layer gel was used.

In SWE breast imaging, small sized ROIs might outperform larger ones (21). However, a lack of standardisation in elastography technique could lead to incorrect stiffness measurement. In the current study, two different sizes of ROI: 1.0 mm diameter and 3.0 mm diameter were used, and the median stiffness values were higher when applying a larger ROI size. One of the possible justifications for these findings was the volume-averaging effect. Larger ROIs have higher probability of covering additional tissues that were close to the fat pad. Therefore, several tissues with more heterogeneous tissue characteristics such as the tendon within the ROI would change the SWV measurements. Our results were consistent with the study by Leong et al (18), in which SWV measurements were found to be higher when using a larger ROI size.

According to previous research, patients should be positioned with their knees flexed in supine position, or in a posture that minimises anisotropy-related abnormalities while stretching the extensor mechanism (29). In this investigation, we manipulated the bovine ankle to maintain both flexed (30 degrees) and neutral positions during scanning. Our results showed that SWV values varied with ankle angle, with slightly lower values observed using CV in the neutral position compared to flexed position. This finding aligns with previous studies reporting that joint positioning can influence tissue biomechanics (30). These variations underscore the importance of standardizing positioning protocols to minimize variability in SWV measurements. While the differences observed in our study were not

statistically significant, we recommend performing scans in the neutral ankle position due to its more consistent SWV values. Although our study showed insignificant differences in SWV when altering the ankle position, we recommend scanning the ankle in a neutral position as the SWV was more consistent.

Based on the confounding factors study, we developed a standard scanning protocol for KFP: scanning acquisition in the longitudinal plane, with use of one-layer ultrasound gel, ROI size of 1.0 mm diameter, and neutral position. Although both operators had vast differences in experience, our study showed good inter-observer reliability. This result was likely due to the use of RMI in the Samsung scanner SWE. RMI is a quality control parameter embedded into the 2-D SWE system. The higher the RMI values, the higher the reproducibility measurements. This parameter could have assisted the operators in filtering out unreliable SWE acquisition and deciding which image was appropriate for use in SWE assessment. This resulted in good inter-observer reliability, as evidenced by the high ICC values seen in our study.

Although SWE has been proven to be a useful for diagnosing MSK disorders, yet, the application could be hampered by technological variations across different manufacturers. In this study, we rescanned the fat pad using two machines from different manufacturers. Our results indicated moderate agreement with no proportional bias. A study by Quantitative Imaging Biomarker Alliance (QIBA) showed at a depth of 3 cm to 7 cm, the poor signal-to-noise ratio of acoustic push pulses and tracking wave in SWE was observed, thus, causing an increase in stiffness measurement bias (31). Given that fat pad is a superficial structure beneath the skin, this justified good agreement and reliability found for fat pad and suggested that Samsung and Canon machine readings were comparable in superficial organs. However, our results were inconsistent with the study by Shin et al. (32), which stated that SWV measurement varied in different machines. One of the possible justifications for this discrepancy is depth. In the Shin et al. study, they measured the phantom at four depths (2, 3, 4 and 5 cm), which were much deeper than the depth in our study. Weakening of the acoustic push pulse and tracking wave could have caused measurement bias.

Some limitations related to this research must be considered. First was the small sample size. Second, we failed to perform the reliability tests on all bovine ankles as four of the ankles had decayed due to mishandling. Third, our measurements were not validated with mechanical validation such as dynamic mechanical analysis. Because the transducer's pressures were administered subjectively, it was difficult to quantitatively assess how they affected pre-compression. Fourth in this study the gender of ankle bovine is the unknown, which may have introduced variability in tissue properties. Lastly, the results of this study were only based on bovine ankles, further clinical studies involving human subjects is necessary.

CONCLUSION

2-D SWE on fat pad is relatively new, therefore, it is essential to determine the potential confounding factors to establish a standard scanning technique for the fat pad. The scanning plane, ROI size, and phantom position showed significant impact on SWV measurements. While the ankle positioning did not significantly affect the SWV measurement, it is suggested to perform scanning in a neutral position. Therefore, when performing a 2-D SWE assessment on fat pad, we recommend the following established protocols based on the clinical experience and data analysis: scanning acquisition in longitudinal plane, using one-layer of ultrasound gel, ROI size set at 1.0 mm diameter and neutral position. This protocol exhibited good inter-observer reliability and moderate inter-machine reliability. The protocol can be considered sufficient to propose preliminary guidelines for clinical scanning using 2-D SWE for KFP.

ACKNOWLEDGEMENTS

The author would like to thank Samsung and Canon for providing the equipment. This study was supported by the Fundamental Research Grant Scheme (FRGS) at Universiti Teknologi MARA (Ref: FRGS/1/2023/SKK06/UITM/02/7).

REFERENCE

1. Vuurberg G, Hoorntje A, Wink LM, Van Der Doelen BF, Van Den Bekerom MP, Dekker R, et al. Diagnosis, treatment, and prevention of ankle sprains: update of an evidence-based clinical guideline. Br. J. Sports Med. 2018 Aug 1;52(15):956-956.https://doi.org/10.1136/bjsports-2017-098106.
2. Zhang Y, Wang X, Wang X, Cao J, Wang H, Zhang F. Allogeneic tendons in the treatment of malunited lateral malleolar avulsion fractures with chronic lateral ankle instability. BMC Musculoskelet. Disord. 2023 Dec;24(1):1-8. https://doi.org/10.1186/s12891-023-06390-1.
3. Pingel J, Petersen MC, Fredberg U, Kjœr SG, Quistorff B, Langberg H, et al. Inflammatory and metabolic alterations of Kager's fat pad in chronic Achilles tendinopathy. PLoS One. 2015 May 21;10(5): e0127811. https://doi.org/10.1371/journal.pone.0127811.
4. Szaro P, Polaczek M, Ciszek B. The Kager's fat pad radiological anatomy revised. Surg. Radiol. Anat. 2021 Jan; 43:79-86. https://doi.org/10.1007/s00276-020-02552-1.
5. Theobald P, Bydder G, Dent C, Nokes L, Pugh N,

Benjamin M. The functional anatomy of Kager's fat pad in relation to retrocalcaneal problems and other hindfoot disorders. J. Anat. 2006 Jan;208(1):91-7. https://doi.org/10.1111/j.1469-7580.2006.00510.x.
6. Ghazzawi A, Theobald P, Pugh N, Byrne C, Nokes L. Quantifying the motion of Kager's fat pad. J. Orthop. Res. 2009 Nov;27(11):1457-60. https://doi.org/10.1002/jor.20900.
7. Tang Y, Cheng S, Yang Y, Xiang X, Wang L, Zhang L, et al. Ultrasound assessment in psoriatic arthritis (PsA) and psoriasis vulgaris (non-PsA): which sites are most commonly involved and what features are more important in PsA? Quant. Imaging Med. Surg. 2020 Jan;10(1):86. https:// doi.10.21037/qims.2019.08.09.
8. Mohamed AA, Eldeeb A, Elkheshen A. Thyroid Nodules: Comparison Between Ultrasound Elastography and FNAC. Al-Azhar Intern. Med. J. 2022 Oct 1;3(10):137-41. https:// doi.10.21608/AIMJ.2022.131552.1902.
9. Toledo MP. Reliability of ultrasound imaging measures of soft tissue stiffness using elastography in the posterior aspect of the leg (master's thesis). https://hdl.handle.net/10652/3416.
10. Dattola A, Altobelli S, Marsico S, Plastina D, Nistico SP, Cavallo A, et al. Hypodermal adipose tissue sonoelastography for monitoring treatment response in patients with plaque psoriasis. Photomed Laser Surg. 2017 Sep 1;35(9):484-91. https://doi.org/10.1089/pho.2016.4261.
11. Taljanovic MS, Gimber LH, Becker GW, Latt LD, Klauser AS, Melville DM, et al. Shear-wave elastography: basic physics and musculoskeletal applications. Radiographics. 2017 May 11;37(3):855-70. https://doi.org/10.1148/rg.2017160116.
12. Heales LJ, Badya R, Ziegenfuss B, Hug F, Coombes JS, van den Hoorn W, et al. Shear-wave velocity of the patellar tendon and quadriceps muscle is increased immediately after maximal eccentric exercise. Eur. J. Appl. Physiol. 2018 Aug; 118:1715-24. https://doi.org/10.1007/s00421-018-3903-2.
13. Theobald P, Byrne C, Oldfield SF, Dowson D, Benjamin M, Dent C, Pugh N, Nokes LD. The Potential Frictional Significance of Kager's Fat Pad.
14. Shaw HM. Structure and function of entheses and enthesis organs. Cardiff University (United Kingdom); 2007.
15. Ercan H, Resch U, Hsu F, Mitulovic G, Bileck A, Gerner C, et al. A practical and analytical comparative study of gel-based top-down and gel-free bottom-up proteomics including unbiased proteoform detection. Cells. 2023 Feb 26;12(5):747. https://doi.org/10.3390/cells12050747.
16. Cosgrove DO, Berg WA, Dorй CJ, Skyba DM, Henry JP, Gay J, et al. Shear wave elastography for breast masses is highly reproducible. Eur Radiol 2012; 22: 1023–1032. https://doi.org/10.1007/s00330-011-2340-y.
17. Konar S, Bolam SM, Coleman B, Dalbeth N, McGlashan SR, Leung S, et al Changes in physiological tendon substrate stiffness have moderate effects on tendon-derived cell growth and immune cell activation. Front. bioeng. biotechnol. 2022 Feb 28; 10:800748. https://doi.org/10.3389/fbioe.2022.800748.
18. Leong SS, Wong JH, Rozalli FI, Yahya F, Tee YC, Yamin LS, et al. 2D shear wave elastography for the assessment of quadriceps entheses—a methodological study. Skelet. Radiol. 2024 Mar;53(3):455-63. https://doi.org/10.1007/s00256-023-04425-1.
19. Gennisson JL, Deffieux T, Macй E, Montaldo G, Fink M, Tanter M. Viscoelastic and anisotropic mechanical properties of in vivo muscle tissue assessed by supersonic shear imaging. Ultrasound Med. Biol. 2010 May 1;36(5):789-801. https://doi.org/10.1016/j.ultrasmedbio.2010.02.013.
20. Eby SF, Song P, Chen S, Chen Q, Greenleaf JF, An KN. Validation of shear wave elastography in skeletal muscle. Journal of biomechanics. 2013 Sep 27;46(14):2381-7. https://doi.org/10.1016/j.jbiomech.2013.07.033.
21. Cortez CD, Hermitte L, Ramain A, Mesmann C, Lefort T, Pialat JB. Ultrasound shear wave velocity in skeletal muscle: a reproducibility study. Diagn. Interv. Imaging. 2016 Jan 1;97(1):71-9. https://doi.org/10.1016/j.diii.2015.05.010.
22. Wang X, Zhu J, Liu Y, Li W, Chen S, Zhang H. Assessment of ultrasound shear wave elastography: An animal ex-vivo study. J. Appl. Clin. Med. Phys. 2023 Apr;24(4): e13924. https://doi.org/10.1002/acm2.13924.
23. Sun Z, Gepner BD, Lee SH, Rigby J, Cottler PS, Hallman JJ, et al. Multidirectional mechanical properties, and constitutive modeling of human adipose tissue under dynamic loading. Acta Biomater. 2021 Jul 15; 129:188-98. https://doi.org/10.1016/j.actbio.2021.05.021.
24. Kot BC, Zhang ZJ, Lee AW, Leung VY, Fu SN. Elastic modulus of muscle and tendon with shear wave ultrasound elastography: variations with different technical settings. https://doi.org/10.1371/journal.pone.0044348.
25. Moon JH, Hwang JY, Park JS, Koh SH, Park SY. Impact of region of interest (ROI) size on the diagnostic performance of shear wave elastography in differentiating solid breast lesions. Acta radiol. 2018 Jun;59(6):657-63. https://doi.org/10.1177/0284185117732097.
26. Alfuraih AM, O'Connor P, Hensor E, Tan AL, Emery P, Wakefield RJ. The effect of unit, depth, and probe load on the reliability of muscle shear wave elastography: Variables affecting reliability of SWE. Journal of Clinical Ultrasound. 2018 Feb;46(2):108-15.
27. Chen PY, Yang TH, Kuo LC, Hsu HY, Su FC, Huang

CC. Evaluation of hand tendon elastic properties during rehabilitation through high-frequency ultrasound shear elastography. IEEE Transactions on Ultrasonics, Ferroelectrics, and Frequency Control. 2021 May 6;68(8):2716-26.

28. Prado-Costa R, Rebelo J, Monteiro-Barroso J, Preto AS. Ultrasound elastography: compression elastography and shear-wave elastography in the assessment of tendon injury. Insights imaging. 2018 Oct;9(5):791-814. https://doi.org/10.1007/s13244-018-0642-1.
29. Bianchi S, Martinoli C. Ultrasound of the musculoskeletal system. Springer Sci. Bus. Media. 2007 Dec 3.
30. Benech N, Aguiar S, Grinspan GA. Monitoring ageing in beef samples using surface wave elastography: A feasibility study. J. Food Eng. 2021 Oct 1; 307:110647. https://doi.org/10.1016/j.jfoodeng.2021.110647.
31. Palmeri M, Nightingale K, Fielding S, Rouze N, Deng Y, Lynch T, et al. RSNA QIBA ultrasound shear wave speed Phase II phantom study in viscoelastic media. In2015 IEEE. Int. Ultrason. Symp. 2015 Oct 21 (pp. 1-4). IEEE. https:// DOI: 10.1109/ULTSYM.2015.0283.
32. Shin HJ, Kim MJ, Kim HY, Roh YH, Lee MJ. Comparison of shear wave velocities on ultrasound elastography between different machines, transducers, and acquisition depths: a phantom study. Eur. Radiol. 2016 Oct; 26:3361-7. https://doi.org/10.1007/s00330-016-4212-y.